Phonon-Assisted Excitonic Recombination Channels Observed in DNA-Wrapped Carbon Nanotubes Using Photoluminescence Spectroscopy

Phonon-Assisted Excitonic Recombination Channels Observed in DNA-Wrapped Carbon Nanotubes Using Photoluminescence Spectroscopy

S. G. Chou,[1] F. Plentz,[2] J. Jiang,[3] R. Saito,[3] D. Nezich,[4] H. B. Ribeiro,[2] A. Jorio,[2] M. A. Pimenta,[2] Ge. G. Samsonidze,[5] A. P. Santos,[6] M. Zheng,[7] G. B. Onoa,[7] E. D. Semke,[7] G. Dresselhaus,[8] and M. S. Dresselhaus[4,5]

[1]*Department of Chemistry, Massachusetts Institute of Technology, Cambridge, Massachusetts 02139-4307, USA*
[2]*Depto. de Física, Universidade Federal de Minas Gerais, Belo Horizonte-MG, 30123-970, Brazil*
[3]*Department of Physics, Tohoku University and CREST JST, Aoba, Sendai, 980-8578, Japan*
[4]*Department of Physics, Massachusetts Institute of Technology, Cambridge, Massachusetts 02139-4307, USA*
[5]*Department of Electrical Engineering and Computer Science, Massachusetts Institute of Technology, Cambridge, Massachusetts 02139-4307, USA*
[6]*Centro de Desenvolvimento da Tecnologia Nuclear, CDTN/CNEN, Belo Horizonte-MG, 30123-970, Brazil*
[7]*DuPont Central Research and Development, Experimental Station, Wilmington, Delaware 19880-0328, USA*
[8]*Francis Bitter Magnet Laboratory, Massachusetts Institute of Technology, Cambridge, Massachusetts 02139-4307, USA*
(Received 8 August 2004; published 1 April 2005)

By using a sample of DNA-wrapped single-wall carbon nanotubes strongly enriched in the $(6, 5)$ nanotube, photoluminescence emissions observed at special excitation energy values were identified with specific mechanisms of phonon-assisted excitonic absorption and recombination processes associated with $(6, 5)$ nanotubes, including one-phonon, two-phonon, and some continuous-luminescence processes. Such detailed processes are not separately identified in three-dimensional semiconducting materials. A general theoretical framework is presented to interpret the experimentally observed phonon-assisted processes in terms of excitonic states.

Over the past few years, photoluminescence spectroscopy (PL) has become an increasingly important technique for the characterization of single-wall carbon nanotubes (SWNT) [1–5]. The ability to probe the electronic structures of a large number of semiconducting SWNTs has made PL a complementary method to resonance Raman spectroscopy (RRS) for the characterization of SWNTs. In most prior PL studies [1–5], the SWNT samples were dispersed in a surfactant solution, excited with a lamp source, and the PL spectra were recorded over the near and far IR spectral regions. In these studies, the strongly luminescent peaks, associated with the ith electronic interband transitions, E_{ii}^S, for different semiconducting SWNTs are compared using excitation or emission contour maps. Besides the optical characterization of nanotube interband transitions, these PL studies show evidence of phonon-assisted PL processes [6–9], especially when the sample is irradiated by an intense light source. Although evidence for such processes has been mentioned in previous reports, only a few phonon-assisted processes have been observed, with no clear identification given for their physical origins.

In the present Letter, PL measurements were carried out on a $(6, 5)$-enriched DNA-wrapped SWNT sample using laser excitation. PL emission peaks associated with the $(6, 5)$ nanotube, photo-excited in an intermediate energy range between the reported E_{22}^S and E_{11}^S transitions of the $(6, 5)$ nanotube, are analyzed and assigned to a number of phonon-assisted optical absorption and energy relaxation mechanisms. Multiple emission peaks associated with the first- and second-order phonon scattering processes were observed, and continuous PL emissions associated with

thermally excited excitonic processes were also observed. Phonon-assisted processes along the elongated absorption profile, associated with phonons both at the Γ point and near the K point, have been identified and studied in detail. A previous theoretical study [10] of the electron-phonon interaction and relaxation rate has interpreted the observed PL features in the $(6, 5)$-enriched sample within the framework of a free carrier band-to-band model. Here, we elaborate on the interpretation of our experimental observations and examine the phonon-assisted processes in terms of excitonic states.

To obtain detailed information about phonon-assisted PL processes, it is highly desirable to have one dominant (n, m) SWNT species in the sample. Using a starting SWNT sample produced from the CoMoCAT process [11], a $(6, 5)$-enriched DNA-wrapped hybrid (DNA-CNT) sample was then prepared using ion exchange chromatography [12]. 30 μL of this fractionated stock solution was dropped onto a sapphire substrate one μL at a time and dried into a thick layer. The sample was excited with different excitation energies using a Ti:sapphire laser, pumped by an Ar^+ laser. The PL emission was collected in a backscattering geometry and was focused onto an InGaAs diode array detection system and a Spex 750M Spectrometer through a microscope objective. A linear interpolation routine [13] in MatLab was used to construct the contour plot shown in Fig. 1(a).

Figure 1(a) shows a two-dimensional (2D) plot of the excitation vs emission energies of the $(6, 5)$-enriched DNA-CNT sample. The PL emission spectra excited at an excitation energy, $E_{\rm ex}$, between 1.43 eV–1.64 eV such
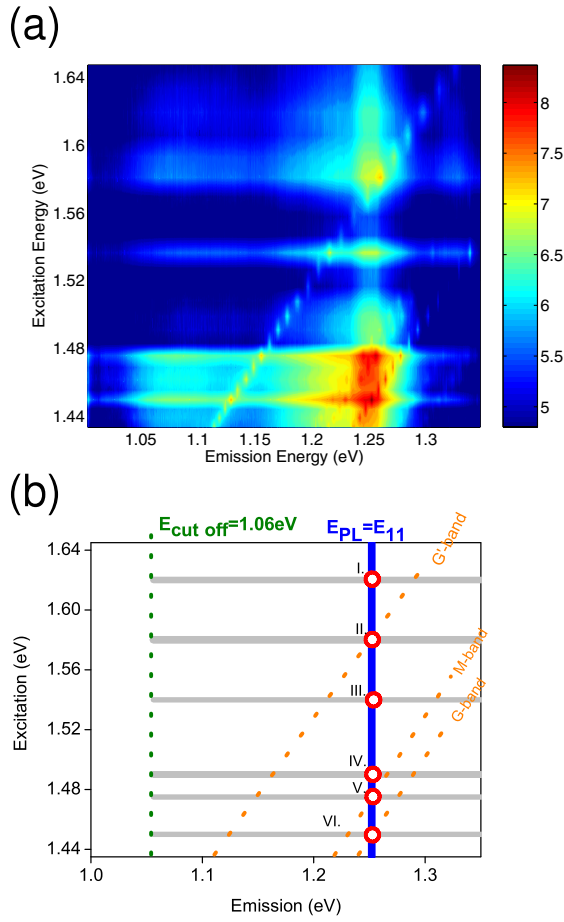
(a)

(b)

FIG. 1 (color online).   (a) A 2D excitation vs emission contour map for a dried (6, 5)-enriched DNA-CNT sample on a sapphire substrate. The spectral intensity is plotted using the log scale shown on the right. (b) A schematic view of the observed PL transitions. The blue vertical band denotes emission at E_{11}^1. The horizontal gray bands denote nearly continuous-luminescence processes associated with thermally excited processes in the different phonon branches. The cutoff energy at 1.06 eV is marked in green. Orange dotted lines denote emission from resonant Raman scattering processes for G-band, M-band, and G'-band phonons. Strong PL emission spots at $E_{11}^1 = 1.26$ eV, denoted by red circles, are associated with one-phonon (VI) and two-phonon (I to V) processes described in Fig. 2 (see text).

that $E_{11}^1 < E_{ex} < E_{22}^1$ ($E_{11}^1 = 1.26$ eV and $E_{22}^1 = 2.19$ eV [3,14]), are recorded in Fig. 1(a) and are labeled in the schematic diagram in Fig. 1(b). The spectral features observed in Fig. 1 can be explained by the different phonon-assisted absorption and recombination processes shown in Fig. 2.

Figure 2 describes the different phonon-assisted processes using the diagrams of the exciton center of mass dispersion relation, $E_{ii}^j(K)$, where E_{ii}^j denotes the ith resonant excitonic subbands of the corresponding bound electron and hole levels, in the jth exciton state, in which $j = 1$ and $j = 2, 3 \dots$ denote the found and excited states of the exciton, and K denotes the exciton crystal momentum. The

solid and open circles denote *real* and *virtual* states, respectively. Optical absorption (excitonic excitation) and emission (radiative recombination) processes occur at $K = 0$ as a result of momentum conservation (with negligible photon momentum). These processes are shown by vertical arrows connecting the excited and ground states. All other arrows, not involving the ground state, denote excitons scattered by phonons.

Previous structurally assigned PL studies [1–5] focused on the SWNT resonant electronic processes described in Fig. 2(a), where absorption of the incident photon occurs at the E_{22}^1 band edge ($a \rightarrow b$). The exciton nonradiatively decays to the E_{11}^1 band edge through multiple channels of relaxation ($b \rightarrow c$) and recombines by emitting a photon ($c \rightarrow a$). The red rectangles labeled with "ex" and "em" correspond to the range of PL excitation and emission energy used in the present experiment. With a strongly enriched SWNT sample and an intense light source, we are able to separately identify the different PL emission peaks associated with specific phonon-assisted processes, as shown in Figs. 2(b)–2(e).

The observed broad range of excitation energies, E_{ex}, accompanied by a narrow PL emission window, corresponds to our general understanding of the PL mechanism, in which an exciton can be excited into a number of excited states before the bound electron-hole pair eventually relaxes to the E_{11}^1 band edge and recombines. Along the E_{ex} scale for the same band edge emission at 1.26 eV in Fig. 1(a), intense PL peaks at several special E_{ex} values were observed. These peaks are shown as red circles in Fig. 1(b). From previous PL studies [3,14], these peaks with the same emission energies can all be correlated with (6, 5) SWNTs, emitting from E_{11}^1. The PL emission for these special red circle E_{ex} values indicated is the most intense at $E_{em} = 1.26$ eV, but is nearly continuous over the range 1.06 to 1.35 eV. These features are labeled by thick, gray horizontal lines numbered from I to VI going across the schematic diagram in Fig. 1(b). Each of the special E_{ex} values is associated with red circles I through V in Fig. 1(b) and can be identified with the two-phonon processes in Fig. 2(b).

In this process, the phonon-assisted absorption can involve the emission of two phonons with opposite momenta, $-q$ ($b \rightarrow c$) and $+q$ ($c \rightarrow d$) [see Fig. 2(b)]. The two-phonon process brings the exciton to the E_{11}^1 band edge, where recombination occurs. The cross section for this process becomes especially large when the E_{ex} values correspond to energies of optical phonon modes that are strongly coupled to the electrons and have a high density of phonon states near the Γ and K points. As a result, the PL emission for the band edge recombination at E_{11}^1 becomes very intense at these special E_{ex} values (such that $E_{ex} = E_{11}^1 + 2\hbar\omega_q$). This two-phonon process gives rise to the intense transitions that are marked by red circles I through V in Fig. 1(b) for different combinations of the Γ point ($q = 0$) and K point ($q = \Gamma K$) optical phonon modes. The

TABLE I.   Assignments of the strong PL spots in Fig. 1 to the different optical phonon branches of the (6, 5) nanotubes

E_{ex} (eV)	Peak Label	Symmetry Point	Phonon Quantity [a]	Phonon Branch
1.62	I	Γ	2	iLO and iTO
1.58	II	K	2	iTO
1.54	III	K	2	iLO and iLA
1.49	IV [b]	K	2	iTA
1.48	V	Γ	2	oTO
1.45	VI	Γ	1	iLO and iTO

[a]1 and 2 refer, respectively, to one- and two-photon processes.
[b]Although a contribution from the combination mode iTO + iLA is also expected around IV, the excitation profile is too broad to distinguish the different processes.
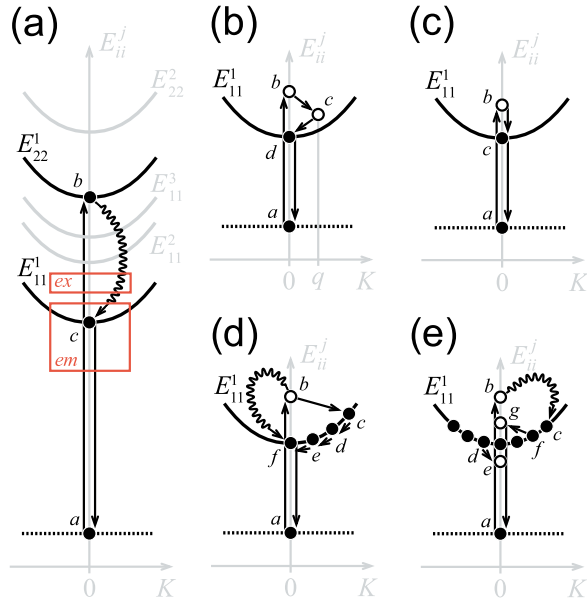
FIG. 2 (color online).   Schematic diagrams for the different phonon-assisted processes (see text). (a) The commonly reported [1–5] excitonic recombination mechanism for the (6, 5) nanotube. The process involves excitonic absorption at E_{22}^1 (point b). The excited exciton can relax down to the E_{11}^1 (point c) via multiple channels, and recombine at E_{11}^1. The red boxes labeled as ex and em, respectively, denote the range of excitation and emission in Fig. 1. Since the excitation range is lower than E_{22}^1, the process shown in (a) is not observed in the present report. The first excited state is estimated as $E_{12}^1 = 1.69$ eV assuming that the exciton binding energies for (6, 5) nanotube scale the same as for (8, 0) nanotube from the first-principle calculations by Spataru *et al.* [24]. (b) Corresponds to the two-phonon-assisted processes responsible for transitions I to V shown in Fig. 1(b). (c) Corresponds to the one-phonon-assisted processes responsible for VI shown in Fig. 1(b). (d) Corresponds to the nearly continuous vertical transitions at $E_{em} = 1.26$ eV. (e) Corresponds to the thermally excited processes that are associated with the horizontal streaks shown across the PL map in Fig. 1(b).

specific energies and assignments of these optical phonon branches are listed in Table I. Furthermore, at $E_{ex} = E_{11}^1 + 0.07$ eV $= 1.33$ eV, strong PL emission is observed for a two-radial-breathing mode (RBM) phonon process [15].

The two-phonon-assisted processes can also occur in a nonresonant fashion. The series of emissions crossing the map diagonally through spots II and V in Fig. 1(b) arise from similar two-phonon M-band and G'-band Raman scattering processes, respectively. Although all SWNTs in the sample contribute to these Raman peaks [orange lines in Fig. 1(b)], especially bright PL peaks are found where these phonon series cross the narrow emission profile of a specific (n, m) SWNT or when the phonon series crosses one of the special E_{ex} values. These Raman scattering peaks mostly occur from nonresonant processes when the phonon series do not cross the E_{11}^1 band edge for the specific (n, m) SWNT in the sample. In the present

experiment, with a (6, 5)-enriched sample, the ~45 ° series become especially intense when the two series cross the strong PL peaks II and V at $E_{em} = 1.26$ eV in Fig. 1(b).

For these phonon series, discrete transitions are observed in Fig. 1(a), because of an experimental artifact instead of the expected continuous transitions diagonally crossing the map. Since only 24 E_{ex} laser lines were used and the experimental linewidths of the Raman transitions are small, the Raman transitions only appear on the map where E_{ex} is equal to one of the 24 E_{ex} values. Since the energy spacings between the successive E_{ex} are large, the linear extrapolation algorithm [13] yields discrete dots rather than a continuous line in Fig. 1(a).

On the other hand, the mechanism associated with VI appearing ~0.2 eV above E_{11}^1 can be explained by a one-phonon process shown in Fig. 2(c). In this process, phonon-assisted light absorption ($a \rightarrow b$) excites the exciton to an excited state. The excitation, along with a simultaneous zone-center ($q = 0$) phonon emission ($b \rightarrow c$), creates an exciton at the E_{11}^1 band edge, where the ground state exciton radiatively recombines ($c \rightarrow a$). This process gives rise to spot VI in Fig. 1 when the G band (the Γ point in-plane optical mode) phonon is emitted. The analogous first-order Raman process that corresponds to the diagonal lines crossing through VI in Fig. 1 corresponds to the G-band Raman scattering peak. Along the diagonal emission series, the Raman process is only resonant when E_{ex} and E_{em} correspond to spot VI and when state "c" is resonant with the E_{11}^1 band edge.

Aside from the special optical phonon states, PL emission is observed at the E_{11}^1 band edge when excited with all E_{ex} values within the range of this experiment, as denoted by the blue vertical stripe in Fig. 1(b). The process is consistent with the general PL mechanism, and the detailed mechanism is depicted by the diagram shown in Fig. 2(d). In this case, light absorption ($a \rightarrow b$) is followed by exciton relaxation to the E_{11}^1 band edge through multiple recombination channels ($b \rightarrow f$, waved arrow). The exciton then radiatively recombines at the E_{11}^1 band edge

$(f \rightarrow a)$. A possible recombination channel, involving the emission of one optical phonon $(b \rightarrow c)$ and several acoustic phonons $(c \rightarrow d \rightarrow e \rightarrow f)$, is shown in Fig. 2(d). Since there are many possible combinations of the initial excited and intermediate states, the excited emission can be continuous with respect to E_{ex}. However, since the phonons involved in such a process do not couple to the electrons as strongly as the optical phonons involved in the processes mentioned in Figs. 2(b) and 2(c), the intensity for such PL emission is weaker.

In connection with the discrete strong PL peaks I through VI mentioned above, the horizontal streaks of continuous emission can be explained by the mechanism shown in Fig. 2(e). In this process, the thermal population of excitons with $K \neq 0$ near the E_{11}^1 band edge is generated by light absorption $(a \rightarrow b)$ and exciton relaxation through multiple recombination channels $(b \rightarrow c$, waved arrow). These $K \neq 0$ excitons can radiatively recombine by either emitting a $q = K$ phonon $(d \rightarrow e \rightarrow a)$ or absorbing a $q = -K$ phonon $(f \rightarrow g \rightarrow a)$ to satisfy the momentum conservation constraint. Such processes contribute to the gray horizontal streaks associated with peaks I to VI shown in Fig. 1(b). The lower energy $(E_{em} < E_{11}^1)$ and higher energy $(E_{em} > E_{11}^1)$ sides of these horizontal streaks correspond to phonon emission $(d \rightarrow e)$ and phonon absorption $(f \rightarrow g)$ processes, respectively. The horizontal streaks only appear for the PL excitation energies near spots I to VI in Fig. 1(b). At these special E_{ex} values, the exciton formation is enhanced by the phonon-assisted absorption processes shown in Figs. 2(b) and 2(c), which increase the $K \neq 0$ exciton population. The assignment of this relaxation mechanism is supported by the observation that the horizontal emission streaks [I through VI in Fig. 1(b)] drop drastically in intensity on the lower energy side of the horizontal streaks at a cutoff energy $E_{em} = E_{11}^1 - \hbar\omega_{max} = 1.06$ eV, where $\hbar\omega_{max} = 0.2$ eV is the largest possible first-order phonon energy for SWNTs and graphite [16]. In this model, low temperature is expected to quench the PL intensity on the higher energy sides of the horizontal streaks, since they are related to the phonon absorption process $(f \rightarrow g)$.

In general, the optical processes discussed in this Letter are difficult to identify separately in solid state systems. For most optical measurements in 3D semiconductors, the phonon and electronic spectra are broad in energy. Moreover, since exciton binding energies of 3D materials are small, detailed phonon-assisted optical processes are not easily observed [17]. On the other hand, by taking advantage of the confinement conditions in low dimensional systems, it is possible to separately identify the different nonradiative processes from optical spectra. Similar phonon-assisted processes have been widely investigated for 0D [18–21] and 2D [21–23] systems, but no systematic studies of such processes have been reported for 1D systems. In this study, we have shown that since

SWNTs are a strongly confined 1D system, the individual phonon-assisted processes in SWNTs can be well resolved, with PL features shown in great detail and over a wide energy range. We have also identified and assigned phonon-assisted excitonic absorption and recombination PL processes observed in the PL spectra for a dried, $(6, 5)$-enriched DNA-CNT hybrid sample, irradiated by an intense excitation source. Strong-two-phonon transitions associated with phonons near the Γ point or the K point were observed at $E_{em} = E_{11}^1$ for selected values of E_{ex}. Resonance Raman processes were observed at $E_{em} = E_{11}^1$, while first- and second-order resonance Raman transitions were observed over a wide range of emission energies. We have shown that by using a SWNT sample highly enriched in a single (n, m) species, one can probe several different phonon-assisted processes not usually separately identified in 3D solid state systems.

[1] M. J. O'Connell *et al.*, Science **297**, 593 (2002).
[2] S. M. Bachilo *et al.*, Science **298**, 2361 (2002).
[3] M. S. Strano, J. Am. Chem. Soc. **125**, 16148 (2003).
[4] M. S. Strano, Nano Lett. **4**, 543 (2004).
[5] Y. Miyauchi *et al.*, Chem. Phys. Lett. **387**, 198 (2004).
[6] J. Lefebvre *et al.*, Phys. Rev. B **70**, 045419 (2004).
[7] J. Lefebvre *et al.*, Phys. Rev. B **69**, 075403 (2004).
[8] J. Lefebvre *et al.*, Appl. Phys. A **78**, 1107 (2004).
[9] H. Htoon *et al.*, Phys. Rev. Lett. **93**, 027401 (2004).
[10] J. Jiang *et al.*, Phys. Rev. B (to be published).
[11] S. M. Bachilo *et al.*, J. Am. Chem. Soc. **125**, 11186 (2003).
[12] M. Zheng *et al.*, J. Am. Chem. Soc. **126**, 15490 (2004).
[13] D. E. Watson, *Contouring: A Guide to the Analysis and Display of Spatial Data* (Pergamon, New York, 1992).
[14] S. G. Chou *et al.*, Chem. Phys. Lett. **397**, 296 (2004).
[15] This two-phonon RBM feature in the PL spectra was observed in a similar $(6, 5)$-enriched DNA-CNT sample in solution in a different experiment.
[16] J. Maultzsch *et al.*, Phys. Rev. Lett. **92**, 075501 (2004).
[17] T. Goto and Y. Nishina, Phys. Rev. B **17**, 4565 (1978).
[18] R. Heitz *et al.*, Phys. Rev. B **64**, 241305(R) (2001).
[19] R. Heitz *et al.*, Phys. Rev. B **56**, 10435 (1997).
[20] H. Benisty *et al.*, Phys. Rev. B **51**, 13281 (1995).
[21] S. Moehl *et al.*, J. Appl. Phys. **93**, 6265 (2003).
[22] H. Zhao *et al.*, Phys. Rev. Lett. **89**, 097401 (2002).
[23] H. Zhao *et al.*, Appl. Phys. Lett. **80**, 1391 (2002).
[24] C. D. Spataru *et al.*, Phys. Rev. Lett. **92**, 077402 (2004).